

AN ABSTRACT OF THE THESIS OF

CHARLES RAY MILES for the degree of MASTER OF SCIENCE

in MECHANICAL ENGINEERING presented on July 13, 1978

TITLE: Modelling and Flow Measurement of Shallow Geothermal

Systems with Downhole Heat Exchangers

Abstract approved:

Redacted for Privacy

Dr. Gordon M. Reistad

The low temperature geothermal deposits in the Klamath Falls area are commonly used for heating buildings. The system often used to accomplish this consists of a heat exchanger that extends the full length of the casing within the well. This casing has slots cut in it to allow geothermal water from the aquifer to circulate through the casing and past the heat exchanger.

A mathematical model for the thermosyphoning in this system was developed. The model was extended to include: a partial-length heat exchanger, the effects of the mixing of the fluid from inside the casing with that from the aquifer, and the effects on heat transfer coefficients caused by the scaling of the casing and heat exchanger. A parametric study of the system showed that the energy extraction

rate from the heat exchanger is largely dependent upon: the temperature of the reservoir, the surface area of the heat exchanger, the ratio of the flow area inside the casing to the area of the annulus between the casing and the well bore, and the degree of mixing between the water from the aquifer and the cooler water from inside the casing.

Flow measurements were made to verify the mathematical model. A hot-film anemometer was used to measure the convective flows within the casing but its use is greatly limited because the coating that protects the hot-film does not hold up at the temperatures encountered in a geothermal well. Construction of an energy balance around the heat exchanger in the well made it possible to estimate the convective flows within the well.

Alternative designs for heat exchangers were examined. A short multi-loop heat exchanger was designed, built, and tested. Initial results indicate that this type of heat exchanger could be used to replace the full-length heat exchangers presently in use for residences.

Modelling and Flow Measurement of Shallow Geothermal
Systems with Downhole Heat Exchangers

by

Charles Ray Miles

A THESIS

submitted to

Oregon State University

in partial fulfillment of
the requirements for the
degree of

Master of Science

Completed July 13, 1978

Commencement June 1979

APPROVED:

Redacted for Privacy

Associate Professor of Mechanical Engineering
in charge of major

Redacted for Privacy

Head of Department of Mechanical Engineering

Redacted for Privacy

Dean of Graduate School

Date thesis is presented July 13, 1978

Typed by Denise Hatfield for Charles Ray Miles

ACKNOWLEDGEMENTS

This project could not have been completed without help, support, and encouragement of many people.

Dr. Gordon Reistad provided much encouragement and valuable advice. I am especially thankful for his support and advice during times when equipment and computer programs were not working properly and for his help during field testing.

David Churchill and David Kreitlow provided valuable information on flow measurements and computer programming.

Masao Fukuda assisted in anemometer calibration and field testing.

Gene Culver at Oregon Institute of Technology had heat exchangers fabricated, prepared wells for testing, and assisted during testing.

Steve Fox assisted in computer programming.

The members of Calvin Presbyterian Church gave me encouragement and much needed spiritual help.

The U.S. Energy Research and Development Administration (now Department of Energy) provided the funding that made this work possible.

TABLE OF CONTENTS

<u>Chapter</u>		<u>Page</u>
I	BACKGROUND INFORMATION AND PRESENTATION OF THE PROBLEM	
	1.1 Introduction	1
	1.2 Types of Geothermal Deposits	1
	1.3 Explanation of DHE System	3
	1.4 Explanation of Total Project	5
	1.5 Tasks to be Performed	7
II	NETWORK MODEL	
	2.1 Initial Work	8
	2.2 Revisions for Short DHE	13
	2.3 Factors Affecting Convective Mass Flow Rate	16
	2.4 Scaling and Mixing	18
	2.5 Influence of Design Variables	21
III	DHE DESIGN AND TESTING	
	3.1 Concept and Advantages of the Short DHE	30
	3.2 Results from Tests in Klamath Falls	31
IV	FLOW MEASUREMENT	
	4.1 Initial Work	38
	4.2 Anemometer Stability	41
	4.3 Energy Balance Method	42
	4.4 Results from Tests in Klamath Falls	45
V	CONCLUSIONS AND RECOMMENDATIONS	
	5.1 Validity of Network Model	50
	5.2 Use of Hot Film Anemometers to Measure Flows in Geothermal Wells	51
	5.3 Performance of Short DHE	52
	BIBLIOGRAPHY	53
	APPENDIX A	55

LIST OF FIGURES

<u>Figure</u>		<u>Page</u>
1.1	Typical DHE System	4
2.1	Network Model for Full-Length DHE	9
2.2	Experimental and Differential Model Predicted Temperature Profiles	10
2.3	Network Model for Partial-Length DHE	14
2.4	Mass Flow Rate for Variations of D/e and D_w about the Standard Set (See Table 2.1)	17
2.5	Experimental and Model Results for Energy Extraction as a Function of Flow Rate Through the DHE. For Well Indicated in Table 2.2	20
2.6	Model Results for Energy Extraction Rate as a Function of Mixing Ratio.	22
2.7	Energy Extraction Rates as a Function of Well Variables D_w and T_s	24
2.8	Energy Extraction Rates as a Function of Well Variables D_c and L	25
2.9	Energy Extraction Rates as a Function of DHE Design Variables \dot{m}_h and Inlet Temperature	27
2.10	Energy Extraction Rates as a Function of DHE Design Variables Number of Loops and XL	28
3.1	Short Multi-Loop DHE	32
4.1	Schematic Diagram of Hot Film Anemometer Bridge	39
4.2	Model for Estimating Convective Flows	43

LIST OF TABLES

<u>Table</u>		<u>Page</u>
2.1	Well Parameters for Well Located at Gibbs Street and Old Fort Road	19
2.2	Design Parameters for Standard Well	23
3.1	Well Characteristics	35

NOMENCLATURE

- A - total area of DHE underwater
- A_c - surface area of casing
- A_e - cross sectional area inside casing with DHE
- A_i - cross sectional area inside casing without DHE
- A_o - cross sectional area of outer annulus
- C_p - specific heat at constant temperature
- D_h - diameter of DHE pipe
- DHE - downhole heat exchanger
- D_c - inside diameter of casing
- D_w - diameter of well bore
- De_e - hydraulic diameter inside casing with DHE
- De_i - hydraulic diameter inside casing without DHE
- De_o - hydraulic diameter of annulus outside the casing
- Ea - anemometer bridge output voltage
- f_{fe} - fanning friction factor for inside casing with DHE
- f_{fi} - fanning friction factor for inside casing without DHE
- f_{fo} - fanning friction factor for outer annulus
- g - acceleration due to gravity
- HR_{ij} - heat flux path ij

L - length of well between perforations

\dot{m} - mass flow rate through casing

\dot{m}_h - mass flow rate through DHE

Pa - power dissipated by hot film sensor

Q - energy extraction rate from DHE

r - fraction of flow through casing that is recirculated

R_1 - control resistance in anemometer electronics

R_2 - $200\Omega \pm 0.1\%$ fixed resistor in anemometer bridge

R_3 - $40\Omega \pm 0.1\%$ fixed resistor in anemometer bridge

R_c - cable resistance for channel 1

R_p - resistance of hot film sensor

T_j - water temperature at node j for network model

T_a - temperature inside casing above DHE

T_b - temperature inside casing above DHE

T_{in} - inlet temperature to DHE

T_{out} - outlet temperature from DHE

T_p - temperature of hot film sensor

T_s - temperature of reservoir

U_e - overall heat transfer coefficient through casing with DHE

U_h - overall heat transfer coefficient through DHE

- U_c - overall heat transfer coefficient through casing without DHE
- w_1 - constant in network convection equation
- w_2 - constant in network convection equation
- w_3 - constant in network convection equation
- XL - length of DHE
- α - ratio of DHE length to total length
- β - thermal expansion coefficient
- ρ - density

I. BACKGROUND INFORMATION AND PRESENTATION OF THE PROBLEM

1.1 Introduction

Downhole heat exchangers (DHE) in geothermal wells have been used for space heating in Klamath Falls, Oregon for many years. The Klamath Falls area represents the largest non-electric use of geothermal energy in the United States and the largest application of the DHE system in the world. There are over 400 geothermal wells in the Klamath Falls area. These wells supply energy for space heating, water heating, and some industrial process heating applications in approximately 500 buildings. However, improvements in the DHE system have occurred through trial and error. The project of which this thesis is a part is one of the first efforts to analytically examine the DHE system.

1.2 Types of Geothermal Deposits

It has been established that approximately 10^{24} Btu of thermal energy lies within 10 kilometers of the surface of the earth. Much of this energy is distributed too diffusely to be easily recovered; however, there are a significant

number of geothermal deposits that are concentrated enough to be of economic interest (1). These deposits may be classified in one of four categories.

a) Hydrothermal convective systems. Water serves as the agent for transferring thermal energy from a deep igneous source to a depth close enough to the surface to be reached by drilling. If the water exists primarily as steam the system is called a vapor-dominated system. If the water is liquid or a saturated liquid-steam mixture the system is called a liquid-dominated system. The geysers in California are a vapor-dominated system and the Salton Sea in California is a liquid-dominated system. There are a very few vapor-dominated systems in the world while liquid-dominated systems are relatively common.

b) Hot igneous system. This system is found in areas of recent volcanic activity. Hot liquid or quasi-liquid rock is close enough to the surface of the earth to be used directly as an energy source. This type of deposit can be found in Hawaii and the Cascade Mountain range. The current level of technology is insufficient to develop this type of system.

c) Impermeable dry rock systems. This system is characterized by unusually large temperature gradients. Thermal

energy is transported from deep within the earth by conduction through solid rock. Los Alamos Scientific Laboratory is currently investigating methods to develop this type of system (2).

d) Geopressured system. This system consists of high-pressure brine which contains dissolved gases. Sand containing water is trapped between layers of impermeable clay. The weight of the material on top of the sand layer pressurizes the system. This type of system often contains significant amounts of natural gas. These systems are found in the Gulf Coast region of the United States on the continental shelf and are currently being developed.

1.3 Explanation of the DHE System

The resource in Klamath Falls is a liquid-dominated convective hydrothermal system. The geothermal brines are generally of low temperature ($< 100^{\circ}\text{C}$) and close to the surface (30m - 250m). This combination makes the use of a DHE system particularly attractive. There are some wells in Klamath Falls that are relatively deep (600m) and do not use the DHE system. DHE systems have been used in Klamath Falls since the 1920's. A typical DHE system is shown in Figure 1.1. Typical dimensions for the system are:

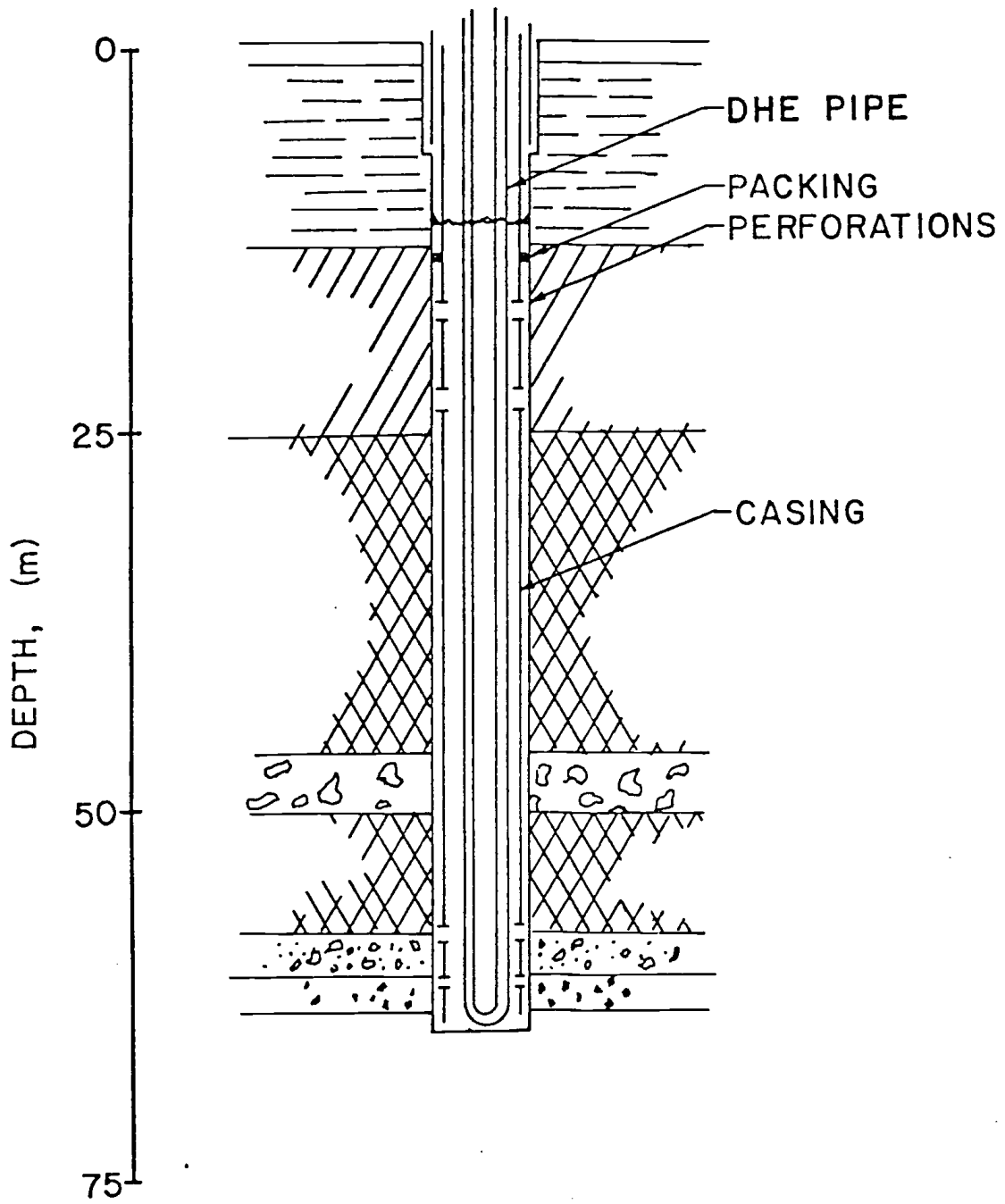


Figure 1.1 Typical DHE system.

well bore	10-12 in.	.254-305m
casing diameter	8 in.	.203m
total depth	250 ft.	77m
water level	45 ft.	14m
length between perforations	160 ft.	50m

The use of the DHE system has several advantages over the extraction of the geothermal brine from the well bore:

a) The water level in the geothermal reservoir is not lowered.

b) The brine does not have to be disposed of at the surface or reinjected.

c) Corrosion is confined to that portion of the DHE that is below the water level in the well.

d) In many cases no external pumping is required because thermosyphoning will pump the secondary fluid through the heat exchanger loop.

1.4 Explanation of the total project

This thesis reports on work that is part of a larger project performed for the U.S. Energy Research and Development Administration (Department of Energy) by Oregon State

University and Oregon Institute of Technology. The overall purpose of the project is three-fold:

a) Determine when DHE systems are feasible both technically and economically.

b) Determine which well parameters have the greater effect on DHE performance.

c) Propose and evaluate improvements in DHE design.

Initially, work on the project was split into two areas: "Flow Measurement" and "Modelling". During the first year these areas were studied by Churchill (3) and Kreitlow (4), respectively. Churchill considered different methods that could be used to measure convective flows within wells. His work indicated that a hot-film anemometer would be a good choice for measuring such flows. An anemometer was purchased, a calibration system for the anemometer was designed and built, the anemometer was extensively calibrated, and some flow measurements were taken in a well without a DHE.

Kreitlow considered mathematical models for the DHE system and investigated the corrosion and scaling effects of geothermal brine on a number of different materials. He developed two models for the energy exchange within the system. His first model was a differential equation model for

the temperature gradients up the well on the inside and outside of the casing and on the down and up legs of the DHE. The equations were solved by integrating from the bottom of the casing to the top perforation level and matching the temperature on the inside and outside of the casing at that point. This model was very sensitive to initial guesses, expensive to run, and difficult to use. In the second model (network model) Kreitlow assumed that the temperature gradients on both sides of the casing were linear. This assumption allowed him to express the governing equations in algebraic form. This model is easy to use, inexpensive to run, and makes it possible to examine the effects of design criteria on well performance.

1.5 Tasks to be Performed

The objectives of the author's research have been:

a) Continue development of the network model and compare results of this model to those of the differential equation model.

b) Continue development of flow measurement techniques and take flow measurements in wells with DHE.

c) Compare the values for velocity within the well obtained by flow measurements to those predicted by the network model.

d) Design a short multi-loop DHE and evaluate its performance.

II. NETWORK MODEL

2.1 Initial Work

The network model is based on the assumption that the temperature gradients up both sides of the casing are linear. With this assumption made, it is possible to model the system as a network with heat and fluid flow paths between the nodes as shown in Figure 2.1. (5) Temperature measurements substantiate the assumption of a linear temperature gradient up the inside of the casing (see Figure 2.2). The governing equations for this network system are as follows:

$$\text{Convective motion: } 2(w_1 + w_2)\dot{m}^2 = T_2 - T_3 \quad (2.1)$$

$$\text{Energy: } T_2 - T_3 = Q/C_p\dot{m} \quad (2.2)$$

$$T_1 - T_3 = Q/C_p\dot{m} - HR_{21}/C_p\dot{m} \quad (2.3)$$

where

$$HR_{21} = \frac{U_i A_c}{2} (T_2 - T_3) \quad (2.4)$$

$$Q = \dot{m}_h C_p (T_{out} - T_{in}) \quad (2.5)$$

$$w_1 = \frac{2f_{fi}}{\rho^2 g A_i^2 De_i \beta} \quad (2.6)$$

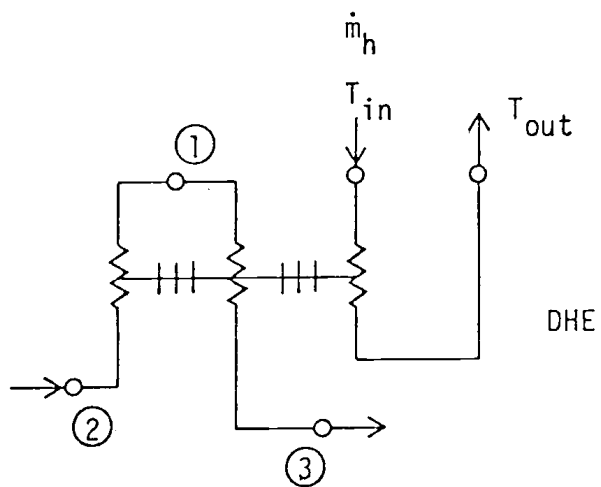
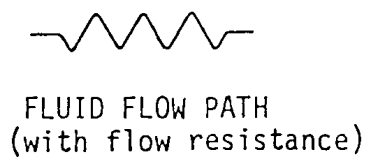
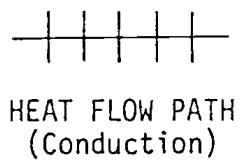


Figure 2.1 Network model for full-length DHE.

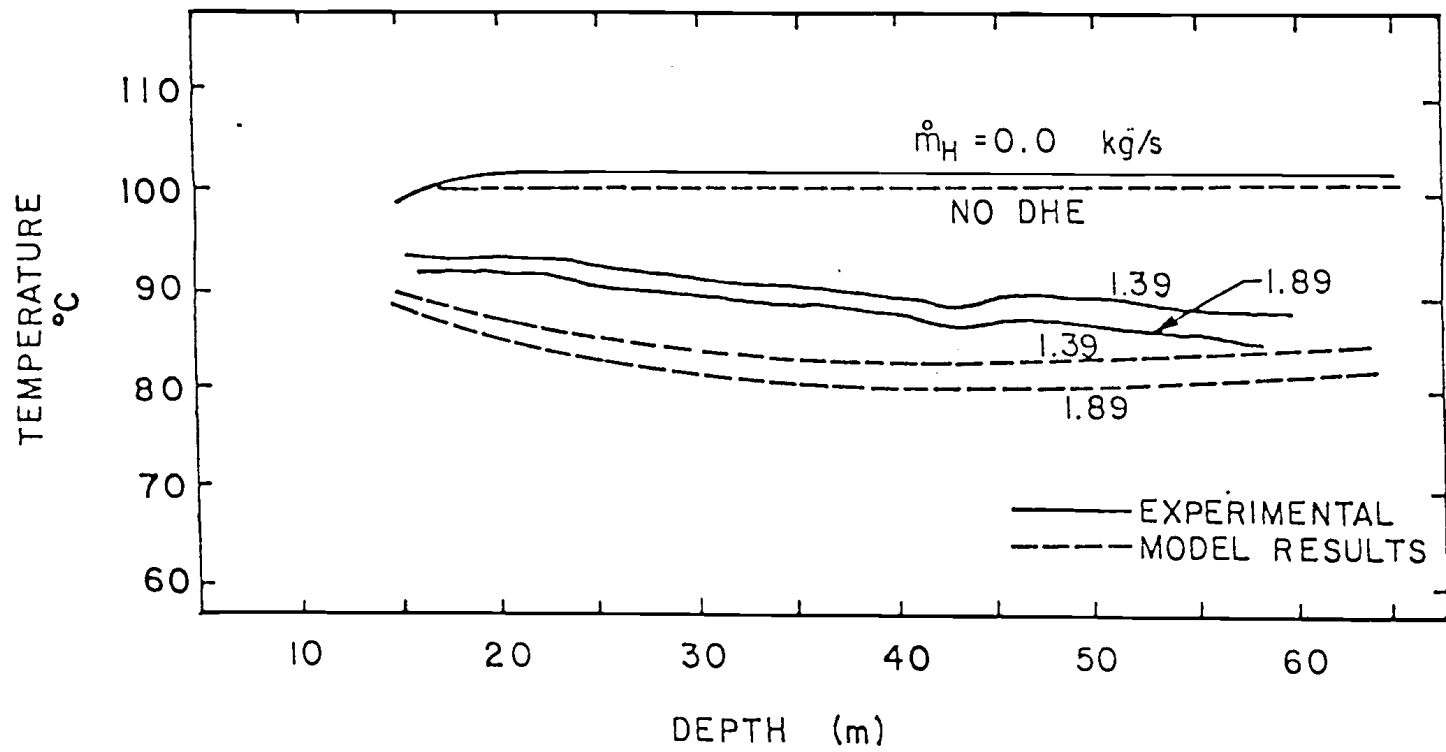


Figure 2.2 Experimental and differential model predicted temperature profiles.

$$w_2 = \frac{2f_{fo}}{\rho^2 g A_o^2 D e_o \beta} \quad (2.7)$$

$$Q = \frac{U_h A}{2} (T_1 + T_3 - T_{in} - T_{out}) \quad (2.8)$$

Combining these equations to give a single equation for \dot{m} gives:

$$\left[\frac{2C_p}{UA} + \frac{1}{\dot{m}_h} \right] \dot{m}^3 + \dot{m}^2 + \frac{U_e A_c}{2C_p} \dot{m} - \frac{T_s - T_{in}}{w_1 + w_2} = 0 \quad (2.9)$$

After \dot{m} is obtained from this equation, the other unknowns are determined by:

$$Q = 2C_p (w_1 + w_2) \dot{m}^3 \quad (2.10)$$

$$T_{out} = T_{in} + Q / \dot{m}_h C_p \quad (2.11)$$

$$T_3 = T_2 - Q / C_p \dot{m} \quad (2.12)$$

$$T_1 = T_2 - \frac{U_i A_c}{2 \dot{m}^2 C_p} Q \quad (2.13)$$

The above model uses the temperature of the reservoir for the temperature of the brine at the bottom of the well outside the casing. However, the perforations at the bottom of the casing would allow the cooler brine from inside the casing to mix with that of the reservoir before it goes up the outside of the casing. The actual temperature of the brine flowing up the outside of the casing would, therefore,

be less than that of the reservoir. If this mixing is taken into account the following equations are added to the governing equations:

$$\text{Mass Conservation: } r \dot{m} + (1-r)\dot{m} = \dot{m} \quad (2.14)$$

$$\text{Energy: } rT_3 + (1-r)T_s = T_2 \quad (2.15)$$

where the mixing ratio (r) is equal to the ratio of the mass flow from inside the casing to the total mass flow rate up the outside of the casing.

If this system of equations is reduced to an equation for the single unknown \dot{m} , the following equation results:

$$\left[\frac{2C_p}{UA} + \frac{1}{\dot{m}_h} \right] \dot{m}^3 + \frac{1+r}{1-r} \dot{m}^2 + \frac{U_e A_c}{2C_p} \dot{m} - \frac{T_2 - T_{in}}{w_1 + w_2} = 0 \quad (2.16)$$

where the terms are as previously defined. When equation (2.16) is solved for \dot{m} , the other unknowns can be determined from the following:

$$Q = 2C_p (w_1 + w_2) \dot{m}^3 \quad (2.17)$$

$$T_{out} = T_{in} + Q / \dot{m}_h C_p \quad (2.18)$$

$$T_2 = T_s - (Q / \dot{m} C_p) \left(\frac{r}{1-r} \right) \quad (2.19)$$

$$T_3 = T_2 - Q / \dot{m} C_p \quad (2.20)$$

$$T_1 = T_2 - \frac{U_1 A_c}{2C_p \dot{m}} (T_2 - T_3) \quad (2.21)$$

2.2 Revision for Short DHE

The model developed by Kreitlow considered only a full length DHE. The model must be modified in order to consider a DHE that does not extend the entire distance from the top to the bottom perforations. A schematic network model for the short DHE system is shown in Figure 2.3. The DHE is assumed to begin at the level of the top perforations and to extend below that point.

The governing equations for this model are:

$$\text{Convective Motion: } \frac{2}{2-\alpha} (w_1 + w_2 + w_3) \dot{m}^2 = T_2 - T_3 \quad (2.22)$$

$$\alpha = \frac{\text{DHE length}}{\text{Total length between perforations}}$$

Energy:

$$T_2 - T_3 = Q/\dot{m} C_p \quad (2.23)$$

$$T_1 - T_3 = (Q - HR_{2-2a} - HR_{2a-1})/\dot{m} C_p \quad (2.24)$$

$$T_1 - T_{1a} = (Q - HR_{2a-1})/\dot{m} C_p \quad (2.25)$$

$$T_2 - T_{2a} = T_3 - T_{1a} = HR_{2-2a}/\dot{m} C_p \quad (2.26)$$

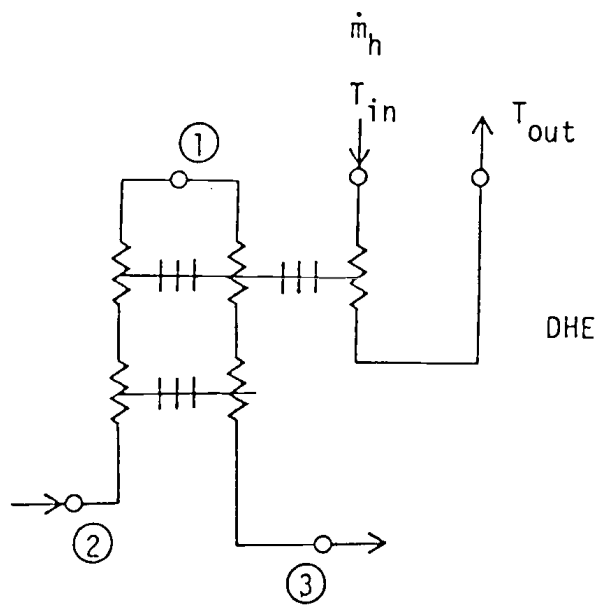
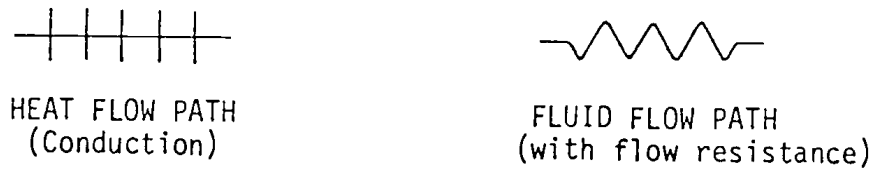


Figure 2.3 Network model for partial-length DHE

where

$$HR_{2a-1} = \frac{U_e A_c \alpha}{2} (T_{2a} - T_{1a}) \quad (2.27)$$

$$HR_{2-2a} = \frac{U_c A_c (1-\alpha)}{2} (T_2 + T_{2a} - T_{1a} - T_3) \quad (2.28)$$

$$Q = \dot{m}_h C_p (T_{out} - T_{in}) \quad (2.29)$$

$$Q = \frac{U_h A_h}{2} (T_1 + T_{1a} - T_{in} - T_{out}) \quad (2.30)$$

$$w_1 = \frac{f_{fo}}{\rho^2 g A_o^2 De_o \beta} \quad (2.31)$$

$$w_2 = \frac{f_{fi}}{\rho^2 g A_i^2 De_i \beta} (1-\alpha) \quad (2.32)$$

$$w_3 = \frac{f_{fe}}{\alpha^2 g A_e^2 De_e \beta} (\alpha) \quad (2.33)$$

Combining these equations to give a single equation

for \dot{m} gives:

$$\left[\frac{2C_p}{U_h A} + \frac{1}{\dot{m}_h} \right] \dot{m}^3 + \dot{m}^2 + \left[\frac{2U_c A_c (1-\alpha)}{C_p} + \frac{U_e A_c \alpha}{2C_p} \right] \dot{m} + (2-\alpha) \frac{T_s - T_{in}}{w_1 + w_2 + w_3} = 0 \quad (2.34)$$

After \dot{m} is obtained from this equation, the other unknowns are determined by:

$$Q = \frac{2C_p}{2-\alpha} (w_1 + w_2 + w_3) \dot{m}^3 \quad (2.35)$$

$$T_{out} = T_{in} + Q / \dot{m}_h C_p \quad (2.36)$$

$$T_3 = T_2 - Q / \dot{m} C_p \quad (2.37)$$

If mixing is included within the model the governing equations must be modified by including equations 2.14 and 2.15. If this set of equations is reduced to an equation for a single unknown \dot{m} , the following equation results:

$$\left[\frac{2C_p}{U_h A} + \frac{1}{\dot{m}_h} \right] \dot{m}^3 + \frac{1+r}{1-r} \dot{m}^2 + \left[\frac{2U_c A_c (1-\alpha)}{C_p} + \frac{U_e A_c (\alpha)}{2C_p} \right] \dot{m} + (2-\alpha) \frac{T_2 - T_{in}}{w_1 + w_2 + w_3} = 0 \quad (2.38)$$

Equations 2.35, 2.36, and 2.37 are unchanged. The computer program used to solve equation 2.38 is presented in Appendix A.

2.3 Factors Affecting Convective Mass Flow Rate

The convective motion governing equation,

$$\frac{2}{2-\alpha} (w_1 + w_2 + w_3) \dot{m}^2 = T_2 - T_3 \quad (2.22)$$

sets the head gain due to buoyancy equal to the head loss due to friction in the convective loop. Model results for the convective flow rate (\dot{m}) through the well of varying D/e ($1/\text{relative roughness}$) of the well bore and D_w (diameter of well bore) are shown in Figure 2.4. These curves show that the convective mass flow rate is very dependent upon the value of D/e as well as D_w .

The values used for D/e and D_w in the model cannot be

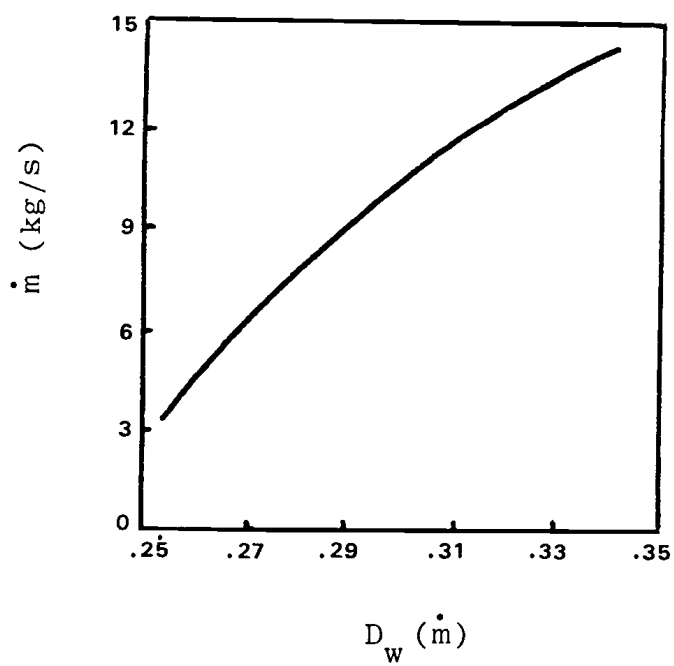
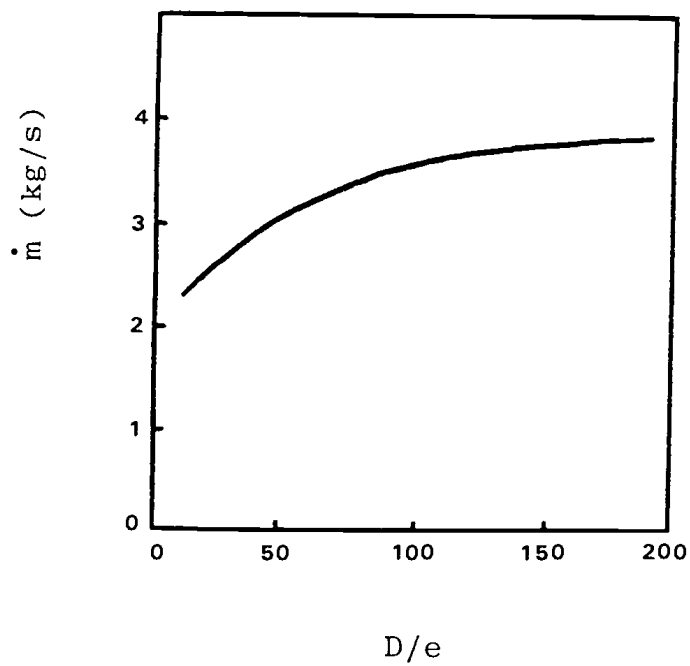


Figure 2.4 Mass flow rate for variations of D/e and D_w about the standard set. (see Table 2.1)

easily measured, therefore, they are estimated.

The author made two estimates for D/e (50 and 100). The value of 100 produced better results when compared to the measured energy extraction rate of a working well. The well characteristics are indicated in Table 2.1 and test results are shown in Figure 2.5. Figure 2.5 also indicates that the well bore for a well drilled with a 10 inch bit probably has a value between 10 and 11 inches. If a well is drilled in a different geological area from Klamath Falls the values of D/e and D_w may be substantially different from those the author used.

2.4 Scaling and Mixing

Scale will be deposited on the portion of the DHE and the casing that are exposed to geothermal brine. This scale will act as an insulating material and will have an effect on the heat transfer within the system. To account for this the overall heat transfer coefficients for the casing and for the DHE were modified as follows:

$$U = \frac{1}{\frac{1}{U} + \frac{1}{U_{\text{scale}}}}$$

A value of $150 \frac{\text{Btu}}{\text{hr-ft}^2\text{-}^\circ\text{F}}$ was used for U_{scale} . (6). The influence of scale on well performance and the selection of design variables will be discussed in Section 2.5.

TABLE 2.1 WELL CHARACTERISTICS FOR WELL
LOCATED AT GIBBS STREET AND
OLD FORT ROAD

WELL BORE (D_w)	.254m
CASING DIAMETER (D_c)	.203m
DHE DIAMETER (D_h)	.060m
NUMBER OF LOOPS	1
LENGTH BETWEEN PERFORATIONS (L)	43m
DHE LENGTH (XL)	43m
TEMPERATURE OF RESERVOIR	101°C
INLET TEMPERATURE TO DHE	21°C

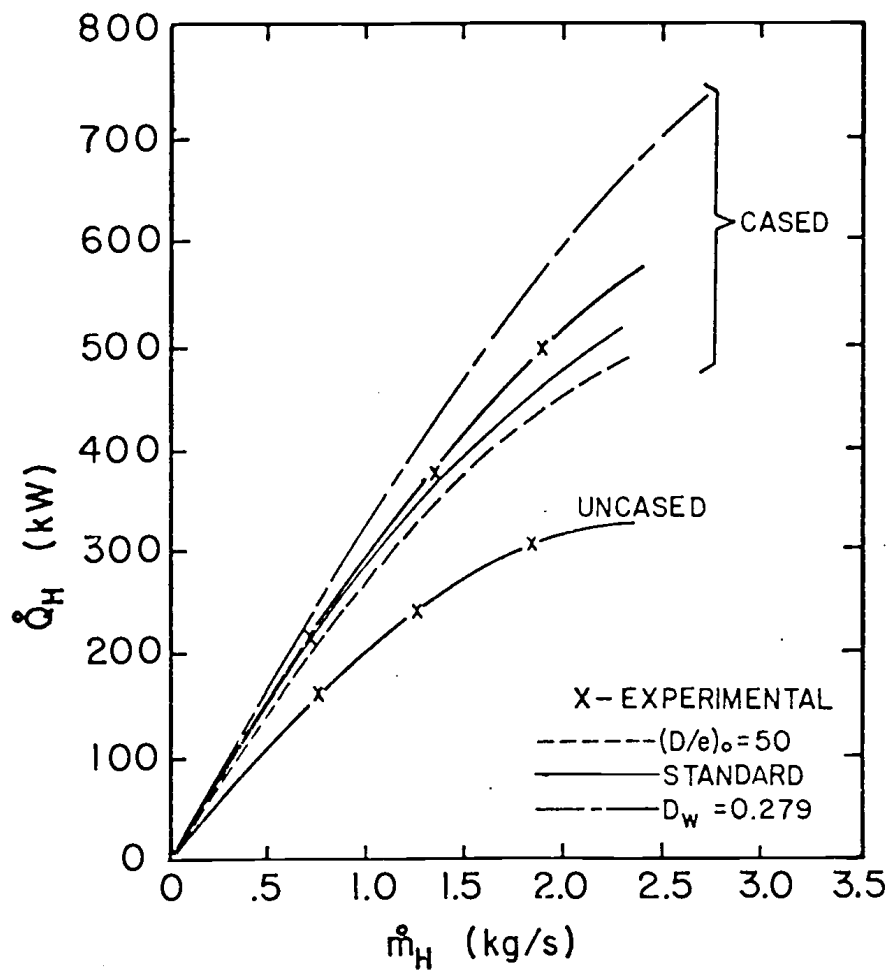


Figure 2.5 Experimental and model results for energy extraction as a function of flow rate through the DHE. For well indicated in Table 2.1.

Mixing of the cooler brine from inside the casing with the brine from the aquifer as it enters the well has a significant effect on well performance. This is shown in Figure 2.6. The decrease in the brine temperature around the DHE caused by mixing is the major factor for the decrease in the energy extraction rate. The degree of mixing is largely dependent on aquifer properties and as yet no good method of estimating the degree of mixing without experimental data has been developed. Methods of calculating the mixing ratio from experimental data are discussed in Section 3.2.

2.5 Influence of Design Variables

To evaluate the effects of design parameters on well performance a set of design criteria for a standard well was established (see Table 2.2), then each parameter was varied while holding the other parameters constant. The parameters considered were well characteristics (D_c , D_w , T_s , and L) and heat exchanger design variables (D_h , XL , number of loops, \dot{m}_h , and inlet temperature).

The influence of the well characteristics are shown in Figures 2.7 a and b and 2.8 a and b. The figures showing the influence of D_w and D_c indicate that the relationship between the area inside the casing and the area of the annulus between the casing and the well bore has a large

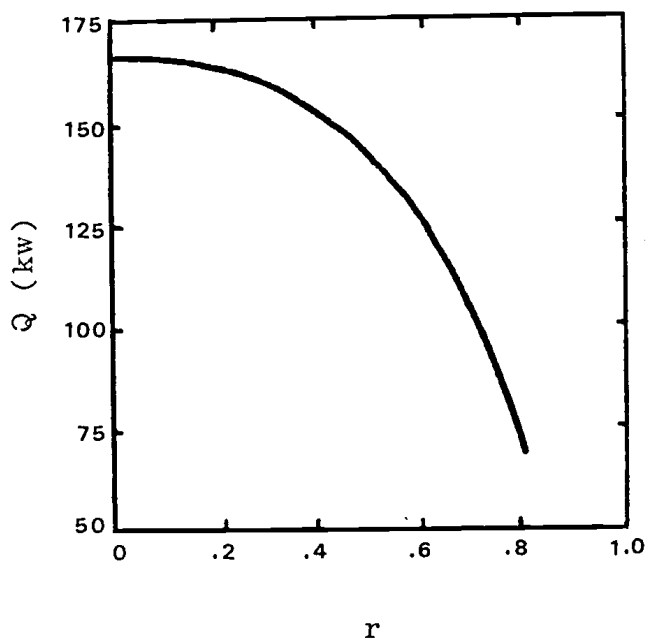


Figure 2.6 Model results for energy extraction rate as a function of mixing ratio. For well indicated in Table 2.2.

TABLE 2.2 DESIGN PARAMETERS FOR STANDARD WELL

WELL BORE (D_w)	.254m
CASING DIAMETER (D_c)	.203m
DHE DIAMETER (D_h)	.060m
NUMBER OF DHE LOOPS	1
LENGTH BETWEEN PERFORATIONS (L)	50m
DHE LENGTH (XL)	50m
MASS FLOW RATE THROUGH DHE (\dot{m}_h)	3.0 kg/sec
TEMPERATURE OF RESERVOIR (T_s)	100°C
INLET TEMPERATURE TO DHE	71°C

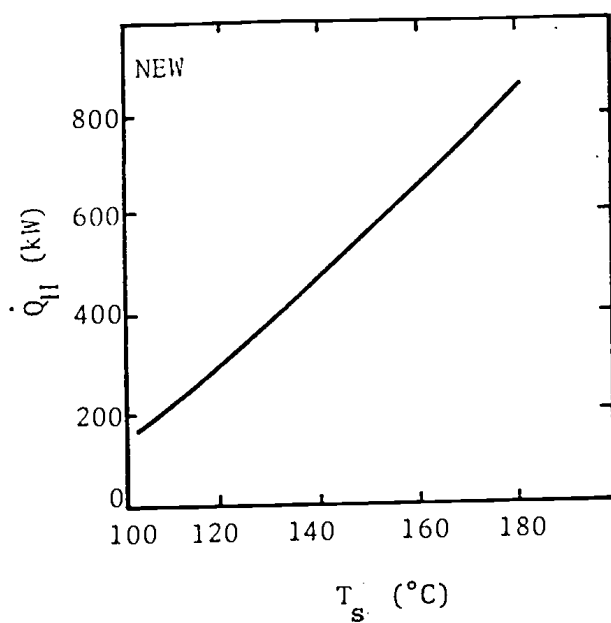
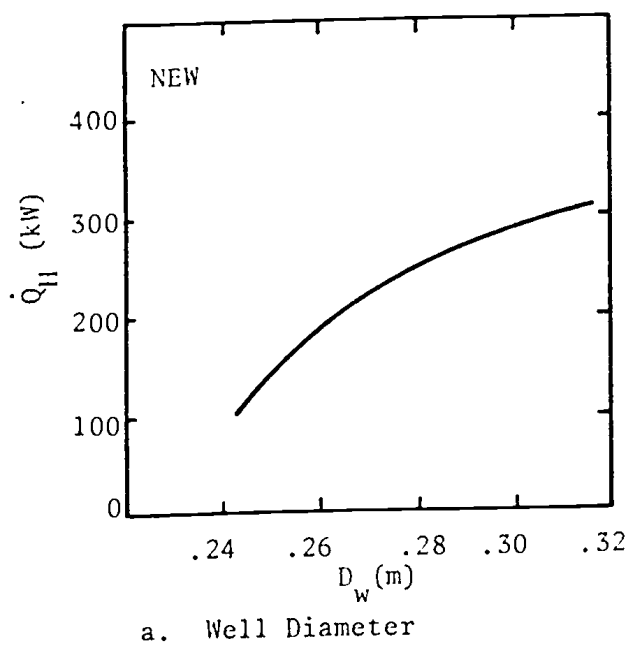


Figure 2.7 Energy extraction rates as a function of well variables D_w and T_s .

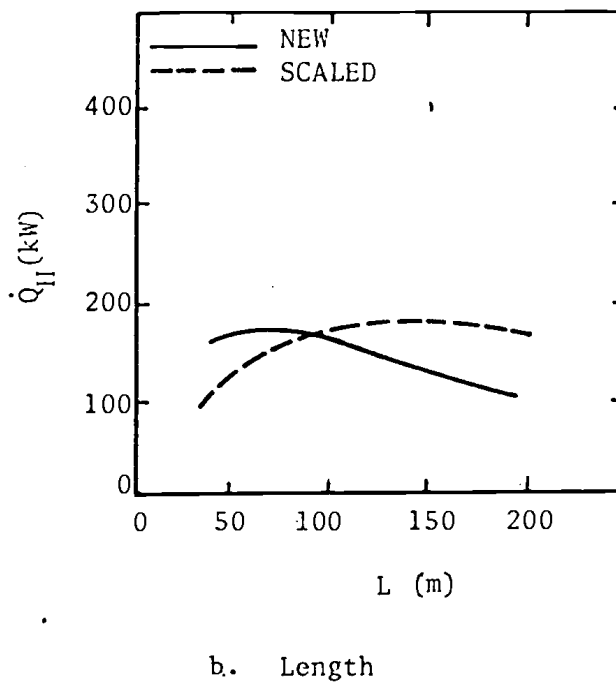
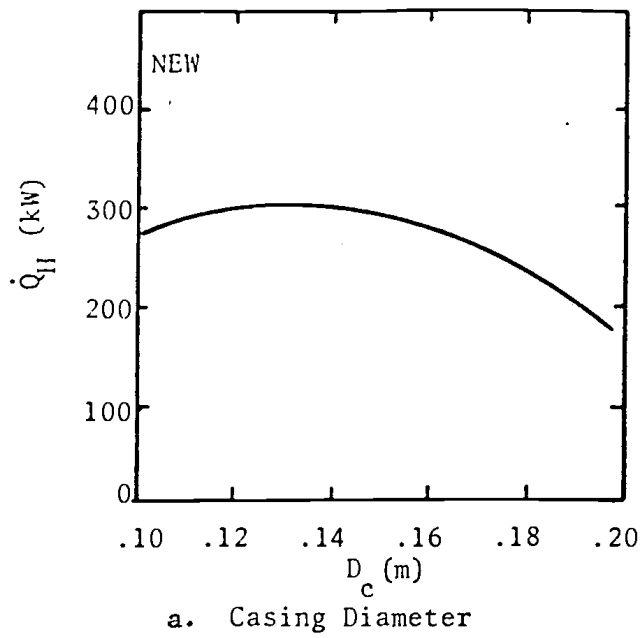
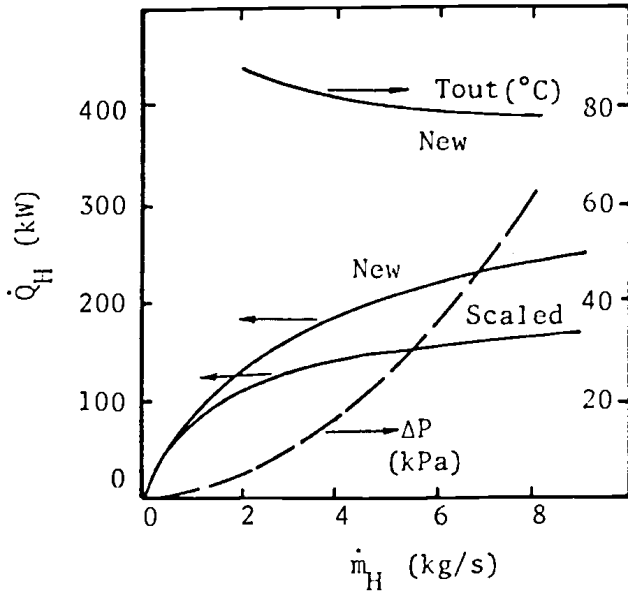


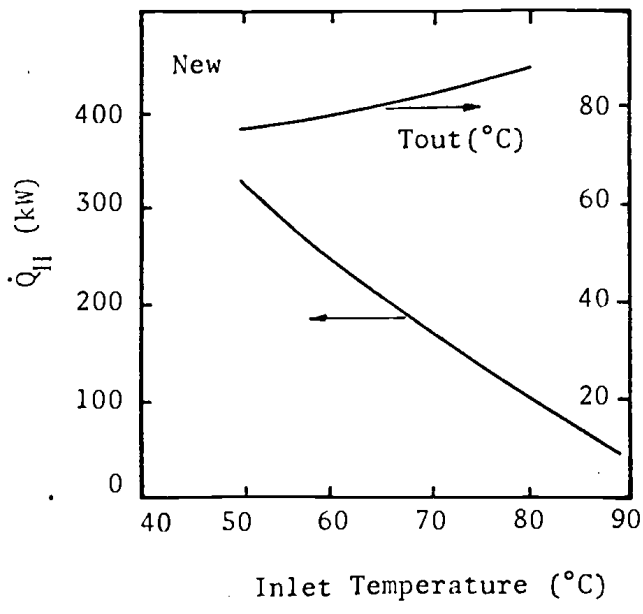
Figure 2.8 Energy extraction rates as a function of well variables D_c and L .

influence on the energy extraction rate. Most wells in the Klamath Falls area are drilled with a 10 inch bit, therefore, the well bore can be assumed to have a diameter of between 10 and 11 inches (see Figure 2.5). Results from the network model indicate that installation of a 6 inch (.152m) casing rather than the standard 8 inch (.203m) casing and a 2 inch (.060m) single loop DHE would increase the energy extraction rate by approximately 50%. Energy extraction rates increase linearly with reservoir temperature (T_s) to a temperature above 200°C . The value of L is normally dependent upon the structure of the aquifer and is not readily controllable. Small or large values for L decrease the performance of the well. For wells that are unusually deep the output could be increased by placing the perforations in the casing at a point farther below the water line. The deposit of scale will tend to flatten the peak of the curve (see Figure 2.8b). The scale will act as insulation thus decreasing the heat transfer through the casing. This will tend to increase the convective flow rate in the well. For larger values of L the effect of this increase in convective flow rate will be greater, than the decrease in the heat transfer coefficient caused by scale on the DHE.

Figure 2.9 a and b and 2.10 a and b show the effect of the heat exchanger design variables. As the DHE area

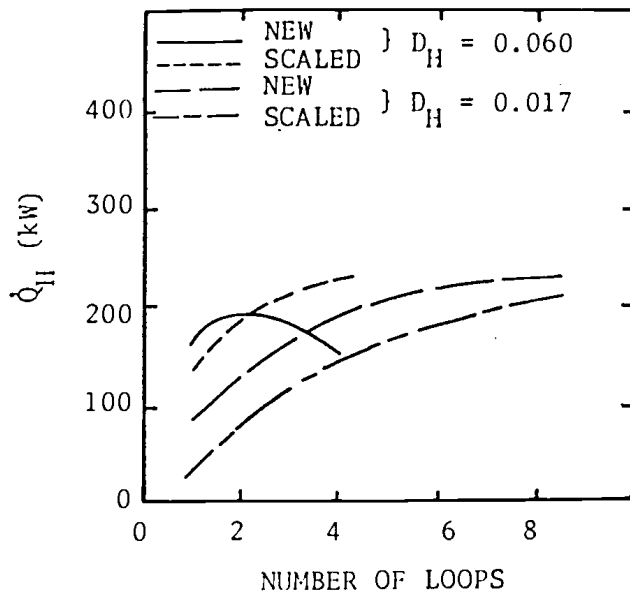


a. Mass Flow Rate

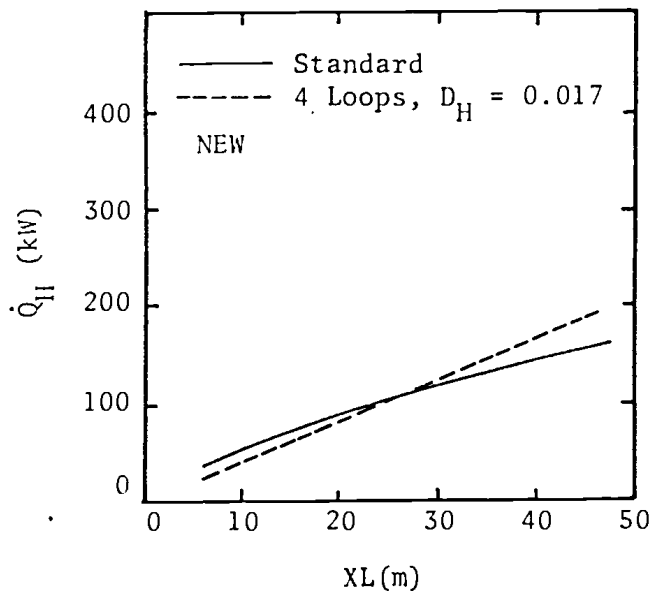


b. Inlet Temperature

Figure 2.9 Energy extraction rates as a function of DHE design variables \dot{m}_h and inlet temperature.



a. Number of loops and heat exchanger tube diameter.



b. Heat Exchanger Length

Figure 2.10 Energy extraction rates as a function of DHE design variables number of loops and XL .

is increased either by increasing the number of loops or by increasing the heat exchanger length (XL) the energy extraction rate will increase. The addition of loops to the DHE will increase the energy extraction rate until the DHE effectively fills the casing and slows the convective flow rate within the well. Again the deposit of scale will tend to flatten the curve. Extraction will increase as the mass flow rate (\dot{m}_h) increases but the pressure drop through the DHE will also increase and the outlet temperature will decrease. If the pressure drop through the DHE becomes too great the secondary fluid will have to be pumped through the DHE because the thermosyphoning effect will be too small. Decreasing the inlet temperature dramatically increases the energy extraction rate but also decreases the outlet temperature.

III. DHE DESIGN AND TESTING

3.1 Concept and Advantages of the Short DHE

DHE systems for a single house in Klamath Falls have design parameters similar to those listed in Table 2.2 with the exception that the mass flow rate through the DHE is typically .6 kg/sec (10 gal/min). This DHE system is over-designed to produce the required energy extraction rate that is needed to heat a single home. The surface area of the DHE could be decreased significantly and still not greatly effect the performance of the system (see Figure 2.9a). The above condition prompted the design of a short multi-loop DHE.

This DHE would deliver sufficient energy to the house without significantly lowering the outlet temperature from the DHE and without the need to pump the secondary fluid through the DHE. The advantages of this type of DHE are:

- a) It requires less material to make.
- b) It may be produced in quantity in a shop and transported to the well.

c) The DHE is lighter, therefore, a smaller crane may be used to install it and it would require less time to install.

A short DHE was designed and fabricated (see Figure 3.1). This DHE was installed in a well and connected to the heating system of a house in November, 1977. The short DHE system provided sufficient energy to heat the house without the need to pump the secondary fluid (7).

3.2 Results From Tests in Klamath Falls

Results from the network model for a well with a full-length DHE have previously been compared to the experimental results from a well with a working DHE in Chapter 2. The results were presented in Figure 2.5. This section presents findings of additional modelling and testing of both full and partial length DHE's.

The energy extraction rates for known flow rates through a full-length DHE were measured for a well at Ponderosa Junior High School. The well was 460 feet (115.4m) deep with a well bore of 14 inches (.36m) and a casing diameter of 12 inches (.30m). The well contained a full-length DHE with two 2 inch loops and one 3 inch loop. The inlet temperature into the DHE was 170°F (77°C) and the flow rates varied from

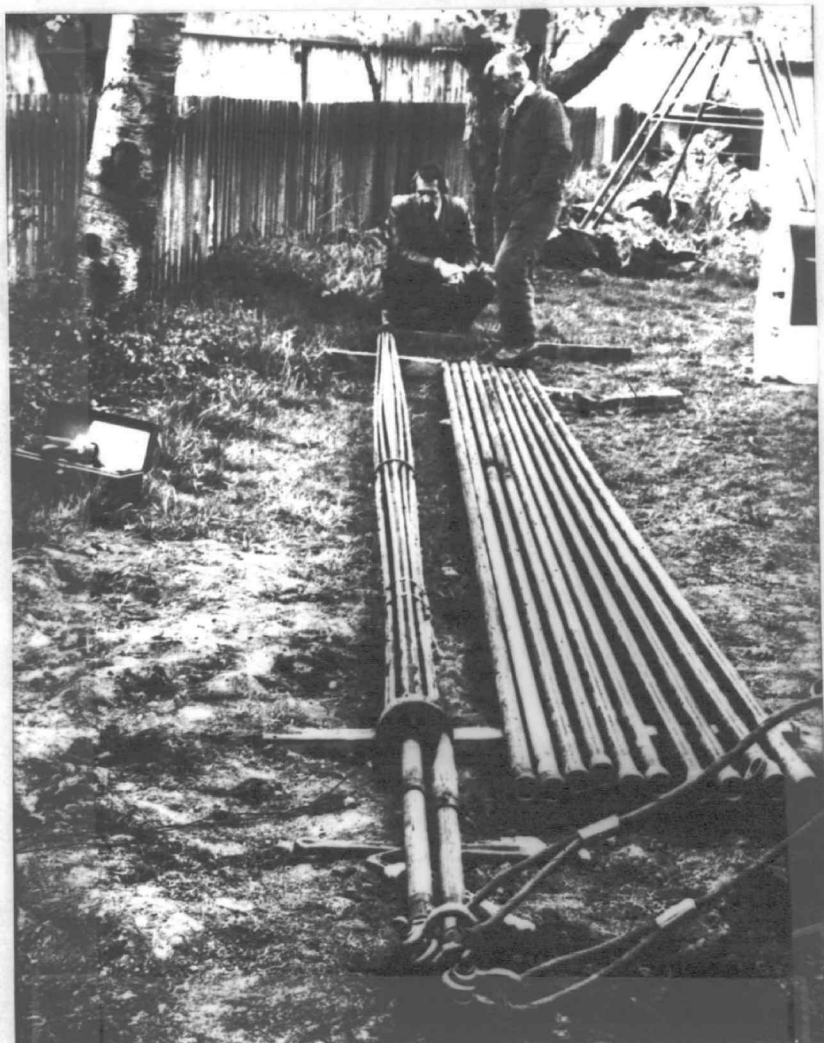


Figure 3.1 Short multi-loop DHE. The length is 21 feet. There are 12, $\frac{3}{8}$ inch pipes and 2, $1\frac{1}{2}$ inch pipes.

240 to 290 gal/min (15 to 20 kg/sec). The mixing ratio was assumed to be zero. The results are summarized as follows:

\dot{m}_h	Q measured	Q model
15 kg/sec	560 kw	599 kw
18 kg/sec	630 kw	638 kw
20 kg/sec	653 kw	660 kw

These results are in good agreement with the network model for a full-length DHE.

Since the network model was greatly modified for the short DHE, the validity of this model must also be experimentally verified. Tests were run on two wells located at 1932 Portland Street and at 2130 Herbert Street in Klamath Falls. The characteristics of these wells are shown in Table 3.1 and the DHE used is shown in Figure 3.1

In May, 1978, measurements were taken at the well located on Portland Street. Input for the model used values of 11 inches (.279m) for D_w and 11 for the number of DHE loops. Since the diameter of the well bore is determined by the composition of the aquifer, the larger well bore is a distinct possibility. The addition of loops to the DHE account for the area of the pipe that is below the waterline in the well but above the DHE. The mixing ratio was estimated

as 0.85 as an average for the four test runs on the well. The method used to estimate the mixing ratio was to estimate the flow rate from the reservoir. The mass flow rate of the brine from the reservoir is obtained from an energy balance of the entire DHE system:

$$\dot{m}_{\text{add}} = \frac{\dot{m}_h (T_{\text{out}} - T_{\text{in}})}{T_s - T_3} \quad (3.1)$$

The mixing ratio can now be calculated:

$$r = 1 - \frac{\dot{m}_{\text{add}}}{\dot{m}} \quad (3.2)$$

The heat transfer results of these measurements are summarized as follows:

\dot{m}_h	Q measured	Q model
.26 kg/sec	59 kw	43 kw
.50 kg/sec	78 kw	71 kw
1.20 kg/sec	147 kw	130 kw
1.80 kg/sec	153 kw	172 kw

The model gave good results for flow rates close to those required to heat a normal house (.6 kg/sec) but slightly under-predicts the energy extraction rates at lower flow rates.

Another series of measurements were taken in June, 1978 at the well located on Herbert Street. Input for the network model used values of 12 inches (.305m) for D_w and 11

TABLE 3.1 WELL CHARACTERISTICS

	Portland Street	Herbert Street
L	64m	46m
D _w	.254m	.267m
D _c	.203m	.203m
T _s	89°C	97°C
D _h	.017m	.017m
XL	6.4m	6.4m

for the number of DHE loops. The mixing ratio was estimated to be 0.5. Temperatures inside and outside the casing could be measured, therefore, the mixing ratio could be calculated by solving Equation 2.15 for r .

$$r = \frac{T_2 - T_s}{T_3 - T_s} \quad (3.3)$$

The results of these measurements are as follows:

\dot{m}_h	Q measured	Q model
.9 kg/sec	170 kw	179 kw
1.35 kg/sec	280 kw	253 kw
1.7 kg/sec	331 kw	307 kw

The predicted energy extraction rates and the measured energy extraction rates are again in good agreement.

Flow conditions in the aquifers appear to be quite different for the two wells. This is indicated not only by the great difference in energy extraction rates from similar wells but also by the time required to reach steady state operating conditions. The well on Portland Street required between $1\frac{1}{2}$ and 2 hours to reach steady state operation when the flow rate through the DHE was changed, while the well on Herbert Street reached a steady state operating condition within 20 minutes. From this it is reasonable to assume that the convective mass flow rate through the well

on Herbert Street is considerably greater than that through the well on Portland Street. This is discussed further in Section 4.4.

IV. FLOW MEASUREMENT

4.1 Initial Work

Churchill's work (8) indicated that a hot film anemometer would be a good instrument to use for measuring flows within this type of geothermal well. The anemometer is used in the constant temperature mode; that is, the temperature difference, between the fluid and the hot film (overheat), is held constant.

The control circuitry for this mode of operation is shown in Figure 4.1. The bridge is in balance when the resistance on both sides are equal.

$$R_1 R_3 = R_2 (R_p + R_c) \quad (4.1)$$

The cable resistance (R_c) is measured on a Wheatstone bridge and the hot film resistance (R_p) is calculated as follows:

$$R_p = a + b T_p \quad (4.2)$$

where a and b are constants and T_p is the desired temperature of the hot film (fluid temperature plus overheat). The constants a and b are obtained by measuring the resistance

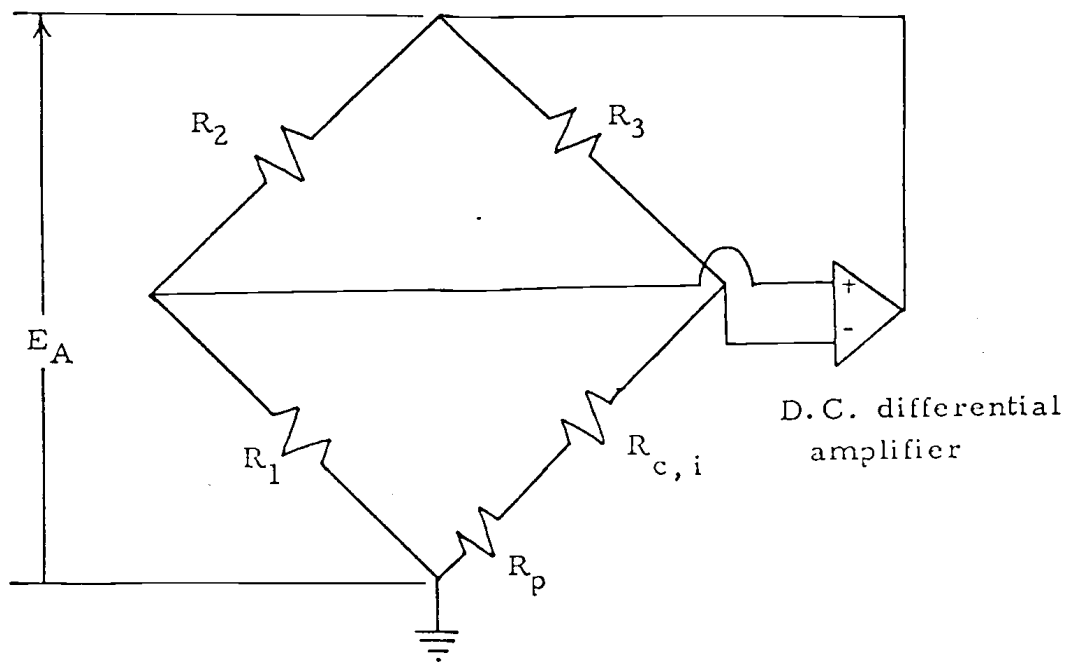


Figure 4.1 Schematic diagram of hot-film anemometer bridge.

of the hot film at several known temperatures and using that data as input for a linear regression analysis. The setting for the variable decade resistor (R_1) is now calculated.

$$R_1 = R_p + R_c \quad (4.3)$$

The other resistances, R_2 and R_3 , are constant at 200Ω and 40Ω , respectively.

The differential amplifier adjusts the current flow through the hot film (R_p) until the bridge is balanced at the desired overheat. The potential across the bridge (E_a) is measured and the power dissipation from the hot film is calculated.

$$P_a = \frac{E_a^2 R_p}{(R_c + R_p + R_3)^2} \quad (4.4)$$

The power dissipation from the hot film is directly proportional to the velocity past the hot film. (9)

Calibration of the anemometer at a given temperature is accomplished by passing water at a known velocity and temperature past the hot film. The variable decade resistance (R_1) is calculated and set. The potential across the bridge (E_a) can now be measured and the power dissipation (P_a) calculated. The required potential (E_a) is measured for several known velocities and a calibration curve (velocity vs. power

dissipation) is plotted for each temperature and overheat.

A single calibration curve is valid only for a given temperature and overheat. The anemometer must be calibrated at or close to the temperature at which it is used. Since temperatures within geothermal wells vary a great deal, a set of calibration curves is required for each value of overheat.

4.2 Anemometer Stability

In January, 1977 the resistance of the probe became unstable. The anemometer was returned to the manufacturer and rebuilt. The rebuilt probe was calibrated and Churchill obtained flow measurements in a well without a DHE. (10) In July, 1977 the resistance of the rebuilt probe became unstable. The author hypothesized that the coating used to electrically isolate the hot film from the brine had separated from the backing and allowed the film to be shorted out. This problem has also been reported by Zakanyz, Wright, and Elrod (11) and by Morrow and Kline (12).

The author tested the coating used by the manufacturer along with several epoxy coatings. This was accomplished by coating a small piece of aluminum, allowing the coating to cure, and placing the piece of metal in hot water (95°C). No coating tested was able to satisfactorily adhere to the

aluminum for a period of 20 hours in the hot water. Since epoxy coatings are difficult to replace the author decided that the coating used by the manufacturer was the best temporary coating that is commonly available. Communications with the manufacturer and several epoxy companies also indicated that there was no commonly available permanent coating that could effectively isolate the hot film in the harsh environment of a geothermal well. The probe could be used for a short time, then the coating would have to be replaced. The manufacturer of the probe would only guarantee the coating for 25 hours of operation and then the coating would have to be replaced. This condition severely limits the allowable calibration and measurement time for a probe.

4.3 Energy Balance Method

The magnitude of the convective flows within the geothermal wells can be estimated by modeling the system as shown in Figure 4.2. The mass flow rate of the convective current can be calculated by taking temperature measurements within the well and the DHE and by making an energy balance. This yields the following relationship:

$$\dot{m}_h (T_{out} - T_{in}) = \dot{m} (T_a - T_b) \quad (4.5)$$

The temperatures above the DHE (T_a) and below the DHE (T_b)

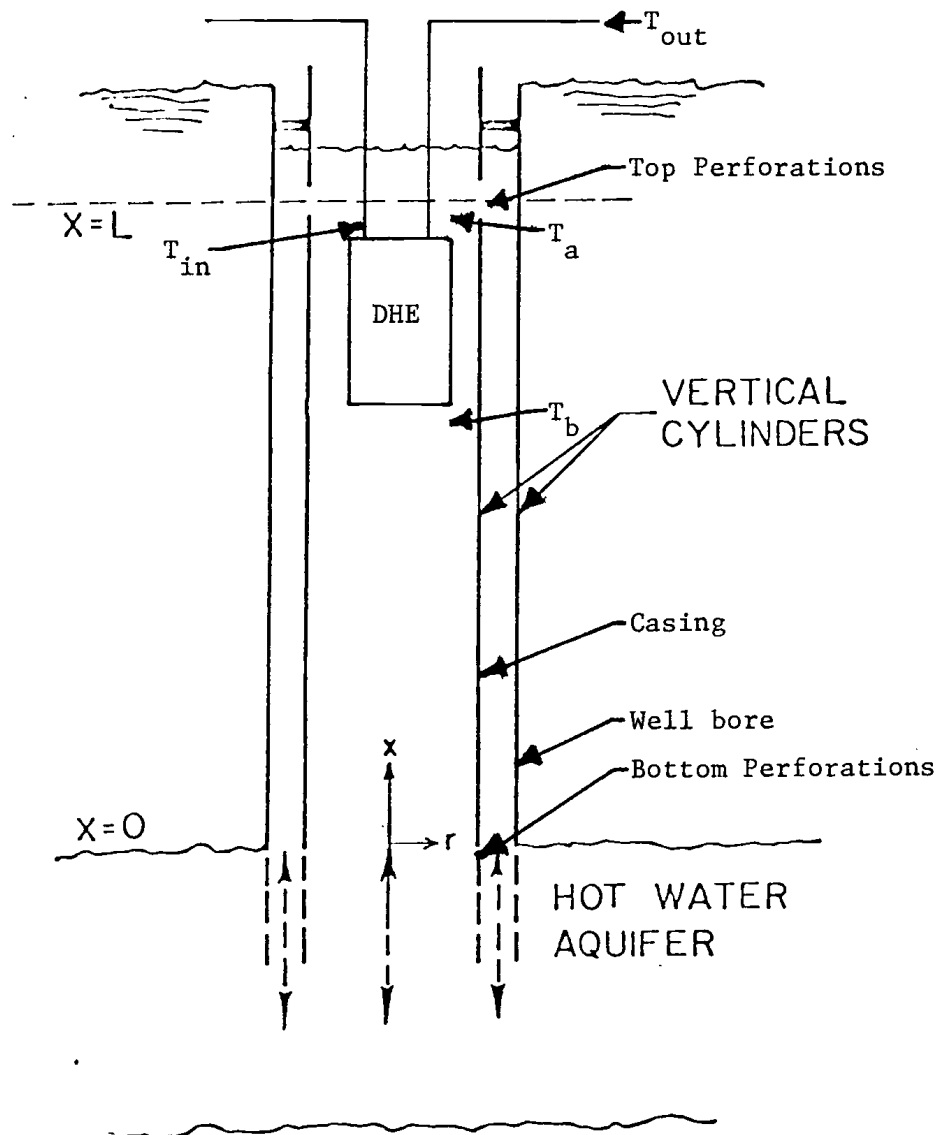


Figure 4.2 Model for estimating convective flows.

are measured with thermistors. The temperature from the DHE (T_{out}) is measured with a thermometer while the inlet temperature to the DHE can be measured with a thermistor located just above the DHE or with a mercury thermometer at the surface. The mass flow rate can be calculated from Equation 4.5:

$$\dot{m} = \frac{\dot{m}_h (T_{out} - T_{in})}{T_a - T_b} \quad (4.6)$$

If a short DHE is used just below the top perforation level, the conduction through the casing can be neglected because the temperature difference between the brine inside the casing and outside the casing is small and the surface area of the casing is relatively small.

If the temperature is measured at the surface, then the temperature in the inlet leg just above the DHE must be estimated. An energy balance for flow through a pipe that is immersed in a fluid of known temperature yields the following relationship:

$$\dot{m}_h C_p (T_B - T_A) = U_p A_p (T_\infty - T_{ave}) \quad (4.7)$$

If T_∞ is much greater than T_B , T_A may be used in lieu of T_{ave} without introducing a significant amount of error. Solving this equation for T_B yields:

$$T_B = \frac{U_p A_p (T_\infty - T_A)}{\dot{m}_h C_p} + T_A \quad (4.8)$$

By evaluating this expression at intervals from the surface to the DHE, the temperature just above the DHE can be estimated.

4.4 Results from Tests in Klamath Falls

Flows have been measured in a well without a DHE by Churchill (13) but not in a well with a working DHE. It is necessary to measure flows in a well with a working DHE not only to determine whether hot-film anemometers can be used to increase this type of flow but also to verify the validity of the network model. Flow measurements were made in the wells located at 1932 Portland Street and 2130 Herbert Street. The flow measurements were conducted simultaneously with the measurement of energy extraction rates discussed in Section 3.2.

In the well located on Portland Street the anemometer was located approximately 2 feet below the top perforations. Results from the anemometer measurements are summarized as follows:

\dot{m}_h	Ea	Pa	Velocity Average
.55 kg/sec	6.05-5.6 volts	.094-.079 w	.76 ft/sec
1.20 kg/sec	5.8-5.6 volts	.090-.084 w	.79 ft/sec
1.80 kg/sec	5.8-5.4 volts	.089-.077 w	.76 ft/sec

The mass flow rate through the casing can be calculated from this velocity. The mass flow rates from the anemometer readings, from the energy balance method, and from the network model are as follows:

\dot{m}_h	\dot{m} anemometer	\dot{m} energy balance	\dot{m} model
.55 kg/sec	7.5 kg/sec	6.3 kg/sec	5.8 kg/sec
1.20 kg/sec	7.6 kg/sec	6.0 kg/sec	7.0 kg/sec
1.80 kg/sec	7.5 kg/sec	7.5 kg/sec	7.6 kg/sec

Here, the inlet temperature into the DHE for the energy balance method was estimated by applying Equation 4.8 at 5 foot intervals from the top of the well, where the temperature was measured, to the top of the DHE. The convective flow rates predicted by the network model are in fairly good agreement with those measured by the anemometer. The results from the energy balance method could be greatly improved by measuring the inlet temperature into the DHE directly instead of having to estimate it.

When measurements were taken at the well on Herbert Street the anemometer was located 2 feet above the top of the DHE but was only about 7 feet below the top perforations.

A thermister was lowered down the inlet side of the DHE to a point just above the DHE, now the inlet temperature could be measured instead of estimated. Results for the flow rates from the energy balance method and the network model are summarized as follows:

\dot{m}_h	\dot{m} energy balance	\dot{m} model
.9 kg/sec	11.1 kg/sec	11.1 kg/sec
1.35 kg/sec	12.3 kg/sec	12.4 kg/sec
1.7 kg/sec	12.9 kg/sec	13.2 kg/sec

The results from the energy balance method and the predictions from the network model are in good agreement.

The coating around the hot-film was cracked after the first set of readings so, readings were obtained only at one heat exchanger flow rate. For this set of readings the potential (E_a) required to balance the anemometer bridge was approximately 8.7 volts, indicating a power dissipation of 0.23 watts. Since the largest power dissipation recorded was 0.07 watts, the experimental reading was too large to allow reasonable extrapolation of the calibration curve. Furthermore, the flow rate calculated from the energy balance would indicate that the power dissipation should have had a value of approximately 0.095 watts. The anemometer appeared to be working properly and was giving consistent

readings, therefore, it is felt that the anemometer reading was not a true indicator of the vertical flow through the casing.

The anemometer was designed so that the hot-film is located on the probe at a position 90° from the stagnation point if the flow is along the tube axis. This was done so that the probe could be used to measure both up and down flows within the casing. At the Reynolds numbers expected boundary layer separation occurs at an angular position of about 80° from the stagnation point. The heat transfer coefficient is at a minimum at the stagnation point and can be as much as 2 times at its maximum which is at the stagnation point. (14) Due to the magnitude of the convective flow and the location of the anemometer (close to the perforations) there could be a significant tangential velocity present. (15) The presence of this tangential velocity makes it impossible to determine the angular position of the hot-film relative to the flow and thus invalidates the calibration done with the hot-film at an angular position of 90° .

Two things can readily be done to correct this condition. First, the anemometer could be placed farther from the top perforations. This would allow the tangential velocity to be damped out. If this is not possible a shroud

could be mounted around the probe so that the flow around the hot-film is always from the same direction. The shroud would have to be small enough to fit down a well but should not restrict the flow to the hot-film. The probe should also be redesigned to relocate the position of the hot-film to the vicinity of the stagnation point.

V. CONCLUSIONS AND RECOMMENDATIONS

5.1 Validity of the Network Model

A network model for the DHE system has been developed and extended to include the partial-length DHE and mixing. The predictions from this model were compared to test data from wells with DHE's installed. The results from these tests indicated that the network model can predict with reasonable accuracy both the energy extraction rate and the magnitude of the convective flow within the well. A parametric analysis showed that the energy extraction rates from the well are largely dependent upon the temperature of the geothermal reservoir, the surface area of the DHE, the ratio of the flow area inside the casing to that of the annulus, and the degree of mixing between the cooler brine from inside the casing and the brine from the aquifer as it enters the well. The magnitude of the convective flows for a given flow rate through the DHE and inlet temperature is largely dependent upon the relative roughness of the well bore and the ratio of the area inside the casing to that of the annulus.

The relative roughness of the well bore, the diameter of the well bore, and the degree of mixing must be estimated and used as inputs for the network model. Limits have been fairly well established for the relative roughness and the diameter of the well bore, but the degree of mixing is largely dependent upon the flow conditions in the aquifer. More experimental data from a variety of wells is needed to more accurately estimate the degree of mixing.

5.2 Use of Hot-Film Anemometers to Measure Flows in Geothermal Wells

A hot-film anemometer can be used to measure flows within geothermal wells but its use is severely limited. The chief limitation is the durability of the probe. The coating that electrically isolates the hot-film from the geothermal brine does not satisfactorily adhere to the backing of the hot-film at the high temperatures encountered in a geothermal well. This coating must be replaced after a short period of use. The replacement of this coating is expensive and time consuming. Output from the anemometer is also sensitive to flow direction.

For the hot-film anemometer to be a dependable flow measuring device for geothermal wells, the problem of electrically isolating the hot-film from the geothermal brine

must be solved. The problems of flow direction around the probe can be solved by locating the probe farther below the top perforations or by placing a shroud around the probe. The probe should be redesigned to locate the hot-film at the stagnation point instead of near the separation point.

5.3 Performance of Short DHE

A short multi-loop DHE was designed and built. This DHE was installed in a well and connected to the heating system of a house. During the first winter of operation it produced satisfactory results. Initial tests on wells with a short DHE tend to indicate that it could be a viable alternative to the full-length DHE for residential use.

More tests are needed to verify the performance of the short multi-loop DHE. An economic analysis should be undertaken to compare the short multi-loop DHE with the full-length DHE.

BIBLIOGRAPHY

1. Tasch, J.H., Geothermal Deposits: Origin Evaluations, and Present Characteristics, Tasch Assoc., Sudbury, Massachusetts, 1976, pp. 1-8.
2. "Annual Report Fiscal Year 1977, Hot Dry Rock Geothermal Energy Development Project", Los Alamos Scientific Laboratory, LA-7109-PR, Los Alamos, New Mexico, 1978.
3. Churchill, David J. "Flow Measurement and Characterization in Shallow Geothermal Systems Used for Downhole Heat Exchanger Applications." Masters Thesis, Oregon State University, 1978.
4. Kreitlow, David B. "Geothermal Well Downhole Heat Exchanger Design Analysis." Masters Thesis, Oregon State University, 1978.
5. Kreitlow, pp. 22-23.
6. Mark's Mechanical Engineers' Handbook, Edited by T. Boumeister, Sixth Edition, 1958, p. 4-106.
7. Svanevik, Larson S., personal communication, May 1, 1978.
8. Churchill, pp. 56-58.
9. "Hot Film and Hot Wire Anemometry, Theory and Application," Thermo Systems Incorporated, Bulletin TB5, St. Paul, n.d.
10. Churchill, pp. 87-116.
11. Zakanycz, S., Wright, H.E., and Elrod, W.C., "Velocity Measurements in Fluids with a Constant Temperature Anemometer," Flow - - It's Measurement and Control in Science and Industry, Vol.2, Instrument Society of America, Pittsburgh, 1974, pp. 571-577.
12. Morrow, T.B., and Kline, J.S., "The Performance of Hot-Wire and Hot-Film Anemometers Used in Water," Flow - - It's Measurement and Control in Science and Industry, Vol. 2, Instrument Society of America, Pittsburgh, 1974, pp. 97-116.

13. Churchill, pp. 97-116.
14. Kreith, Frank, Principles of Heat Transfer, International Textbook Company, Scranton, pp. 408-410.
15. Baker, D.W., and Sayre, Jr., C.L., "Decay of Swirling Turbulent Flow of Incompressible Fluids in Long Pipes," Flow - - It's Measurement and Control in Science and Industry, Vol. 1, Instrument Society of America, Pittsburg, 1974, pp. 301-312.
16. Culver, G.G., Fukuda, M., Kreitlow, D.B., and Reistad, G.M., "Natural Convection Heat Transfer Models for Downhole Heat Exchanger Applications in Shallow Geothermal Systems," ASME Paper No. 77-HT-55, April, 1977.
17. Kays, W.M., Convective Heat and Mass Transfer, McGraw-Hill, New York, 1966.
18. Welty, J.R., Wicks, C.E., and Wilson, R.E., Fundamentals of Momentum, Heat and Mass Transfer, Wiley, New York, 1969.

APPENDIX A

Computer program to solve Equation 2.38

This program solves the equation for the network model that was presented as Equation 2.38. The program is designed to be run interactively from a time-sharing terminal. The results are written on tape 7 and may be routed to the line printer.

```

PROGRAM MAIN(INPUT,OUTPUT,TAPE7,TAPE8=OUTPUT)
IMPLICIT REAL (L,M)
COMMON/ONE/AD,A1,A2,A3,A,AC,AI,AO,AF,B,DC,DEE,DEI,DEC,OH,OLN,OW
COMMON/TWO/XL,FN,FEFF,FEI,FFE,FFO,HI,H4,L,M,HH,TH,TN,TIN,TS,HE
1,T3,O1,O2,CP,iOLT

COMMON/THREE/U,UC,W1,W2,W3,ALPHT,UCF,PLF(100,2),PI,RP,PSI
COMMON/FOUR/FFH,VI,VE,VFE,VO,Q,QMAX,EFF,COSKWH,FNGY
DATA MDOT/4./

C
C   READ DATA
C
10 CALL READ1(J,STEP,NS)

C
C   PUT HEADING ON FILE
C
WRITE(7,11)
11 FORMAT(5X,#DC#,T14,#OH#,T23,#OH#,T32,#TH#,T41,#FIN#,T49,
1#TOUT#,T59,#TS#,T68,#M4#,T77,#M#,T84,#XL#,T91,#L#,T100,
2#Q#,T106,#EFF#,T115,#PSI#,T121,#COSKWH#,T131,#ENGY#)

C
C   CALCULATE AREAS AND EQUIVALENT DIAMETERS
C
DO 100 I=1,NS
NR=I
XL=L*ALPHT
CALL AD

C
C   ASSUME MDOT
C
20 CONTINUE
M=MDOT

C
C   CALCULATE VELOCITIES, REYNOLDS NUMBERS AND FRICTION
C   FACTORS.
C
CALL VRF

C
C   CALCULATE HT COEFFICIENTS
C
CALL HTCDEF

C
C   CALCULATE W1 AND W2
C
CALL WS

C
C   FIN CALCULATIONS
C
CALL FINS

C
C   CALCULATE COEFFICIENTS
C
CALL COEFS

C
C   SOLVE EQUATION
C
CALL SOLVE(A0,A1,A2,A3,M)

C
C   TEST ASSUMED MDOT
C
ERR=ABS(MDOT-M)

```

```

      MODT=M
      IF(LRP/M.GT.0005)GO TO 20
C
      CALCULATE OUTPUT
C
      Q=(2./(2.-ALPHT))*(W1+W2+W3)*4.2*M**3
      TOUT=TIN+Q/MH/4.2
      T3=TS-Q/(M*4.2)*(RM/(1.-RM))
      O1=TS-TOUT
      O2=T3-TIN
      IF(O1.LT.0..OP.O2.LT.0.) GO TO 102
      OMAX=4.2*MH*(TS-TIN)
      EFF=Q/OMAX
C
      CALCULATE COST
      ALWEL=13.8
      ALPIP=9.1
      FROM=.1
      FLF=.2
      CWELL=(226.*OW+30.)*(L+10.)/ALWEL
      CPIPE=((0.89*DH+6.13)*2.*XL+25.*TN)/ALPIP
      COSYR=(CWELL+CPIPE)*(1.+FROM)
      ENGY=Q*FLF*8760.
      COSKWH=100.*COSYR/ENGY
      PLT(I,2)=0
C
      DISPLAY RESULTS
C
      CALL OUTPUT(J,NS)
C
      INCREMENT SELECTED VARIABLE
C
      GO TO (91,92,93,94,95,96,97,98,99),J
91  PLT(I,1)=TIN
      TIN=TIN+STEP
      GO TO 100
92  PLT(I,1)=TS
      TS=TS+STEP
      GO TO 100
93  PLT(I,1)=MH
      MH=MH+STEP
      GO TO 100
94  PLT(I,1)=L
      L=L+STEP
      GO TO 100
95  PLT(I,1)=TN
      TN=TN+STEP
      GO TO 100
96  PLT(I,1)=ALPHT
      ALPHT=ALPHT+STEP
      GO TO 100
97  PLT(I,1)=OW
      OW=OW+STEP
      GO TO 100
98  PLT(I,1)=DC
      DC=DC+STEP
      GO TO 100
99  PLT(I,1)=RM

```

```

      RH=RM*STEP
100 CONTINUE
C
C          PLOT RESULTS
C
102 CALL PLOT(J,NR)
C
      GO TO 10
      END
C
      SUBROUTINE READ1(J,STEP,NS)
      IMPLICIT REAL (L,M)
      COMMON/ONE/A0,A1,A2,A3,A,AC,AI,A0,AE,B,DC,DEE,DEI,DEO,DH,DLN,DW
      COMMON/TWO/XL,FN,FEFF,FFI,FFE,FFO,HI,HH,L,M,MH,TH,TN,TIN,TS,HE
1,T3,D1,D2,CP,TOUT
      COMMON/THREE/U,UC,W1,W2,W3,ALPHT,UCE,PLT(100,2),DI,RM,PSI
C
      DIMENSIONS USED IN PROGRAM
      MASS FLOW RATES ARE IN KG/SEC
      TEMPERATURES ARE IN DEGREES CENTIGRADE
      LENGTHS AND DIAMETERS ARE IN METERS
C
C
C
C
      PRINT*,#ENTER CASING DIAMETER,DHE DIAMETER, MASSFLOW RATE#,
1#THROUGH DHE, AND LENGTH#
      READ*,DC,DH,MH,L
      IF(DC.LE.0.)STOP
      PRINT*,#ENTER INLET TEMPERATURE TO DHE AND #,
1#RESERVOIR TEMPERATURE#
      READ*,TIN,TS
      PRINT*,#ENTER WELL DIAMETER , MIXING RATIO , AND#,
1#RATIO OF DHE LENGTH TO TOTAL LENGTH#
      READ*,DW,PH,ALPHT
      PRINT*,#ENTER NUMBER OF FINS,THICKNESS,LENGTH AND NUMBER OF#,
1# LOOPS#
      READ*,FN,DLN,B,TN
      PRINT*,# ENTER VAR NUMBER,STEP SIZE AND NUMBER OF STEPS#
      PRINT*,# VAR 1= TIN, 2=TS, 3=MH, 4=L, 5=TN, 6=ALPHT#
      PRINT*,#          7=DW, 8=DC, 9=MR#
      READ*,J,STEP,NS
C
      RETURN
      END
C
      SUBROUTINE AD
      IMPLICIT REAL (L,M)
      COMMON/ONE/A0,A1,A2,A3,A,AC,AI,A0,AE,B,DC,DEE,DEI,DEO,DH,DLN,DW
      COMMON/TWO/XL,FN,FEFF,FFI,FFE,FFO,HI,HH,L,M,MH,TH,TN,TIN,TS,HE
1,T3,D1,D2,CP,TOUT
      COMMON/THREE/U,UC,W1,W2,W3,ALPHT,UCE,PLT(100,2),DI,RM,PSI
      DATA TH/.0079/
      PI=4.*ATAN(1.0)
      A=2.*PI*DH*XL*TN
      AC=PI*DC*L
      AI=PI*DC*DC/4
      AO=PI*(DW*DW-(DC+2.*TH)**2)/4.
      AE=PI*(DC*DC-2.*TH*DH*DH)/4.
      PEE=PI*(DC+2.*TH*DH)
      DEE=4.*AE/PEE
      PEI=PI*DC
      PEO=PI*(DW+(DC+2.*TH))

```

```

DEI=4.*AI/PEI
DEO=4.*AO/PEO
RETURN
END

```

C

```

SUBROUTINE VRF
IMPLICIT REAL (L,M)
COMMON/ONE/A0,A1,A2,A3,A,AC,AI,AO,AE,B,DC,DEE,DEI,DEO,DH,DLN,DM
COMMON/TWO/XL,FX,FEFF,FFI,FFE,FFO,HI,HH,L,M,MH,TH,TN,TIN,TS,HE
1,T3,D1,D2,CP,TOUT
COMMON/THREE/U,UC,W1,W2,W3,ALPHT,UCE,PLT(100,2),DI,RM,PSI
COMMON/FOUR/FFH,VI,VE,VHE,VO
DATA RLRFO/100./
DATA RHO,ANU/1000.,.294E-6/
PI=4.*ATAN(1.)

```

C

C

C

```

CALCULATE FLOW VELOCITIES

```

```

VI=M/(RHO*AI)
VE=M/(RHO*AE)
WT=.0026
IF(DH.GT..0267)WT=.0036
IF(DH.GT..154)WT=.0055
VHE=4.*MH/(RHO*PI*(DH-2.*WT)*(DH-2.*WT)*TN)
VO=M/(RHO*AO)
DI=DH-2.*WT
VR=VI/VO

```

C

C

C

```

CALCULATE REYNOLDS NUMBERS

```

```

REO=DEO*VO/ANU
REE=DEE*VE/ANU
REI=DEI*VI/ANU
REH=DI*VHE/ANU

```

C

C

C

```

CALCULATE FRICTION FACTORS

```

```

RLRFI=DEI/.000046
RLRFE=DEE/.000046
RLRFH=DI/.000046
FFI=FFF(REI,RLRFI)
FFE=FPF(REE,RLRFE)
FFH=FRF(REH,RLRFH)
FFO=FPF(REO,PLRFO)
PSI=VHE*VHE/2./9.81*2.*XL/DI*FFH*1.417
RETURN
END

```

C

C

C

C

C

```

FUNCTION FRF(KE,PLRF)

```

```

FUNCTION FRF DETERMINES FRICTION FACTORS

```

```

FF=.01
I=1
IF(RF.LT.2300.)GO TO 300
IF(RE.GT.1.E6)GO TO 200

```

C

C

C

C

C

```

10 FN=4.*ALOG10(PLRF)+2.28-4.*ALOG10(4.67*PLRF/(RE*SQRT(FF))+1.)
FN=1./(FN*FN)
IF(ABS(FN-FF).LT.1.E-5)GO TO 100
I=I+1

```

```

      FF=FN
      GO TO 10
100  IF (RLFF/(RE*SQRT(FF)).GT..01)GO TO 400
200  FF=1./(4.*ALOG10(RLRF)+2.28)**2
      GO TO 400
300  FF=16./RE
400  FRF=FF
      RETURN
      END

```

C

```

SUBROUTINE HTCOEF
IMPLICIT REAL (L,M)
COMMON/ONE/A0,A1,A2,A3,A,AC,AI,AO,AE,B,DC,DEE,DEI,DEO,DH,DLN,DM
COMMON/TWO/XL,FN,FEFF,FFI,FFE,FFO,HI,HH,L,M,MH,TH,TN,TIN,TS,HE
1,T3,D1,D2,CP,TOUT
COMMON/THREE/U,UC,W1,W2,W3,ALPHT,UCF,PLT(100,2),DI,RM,PSI
COMMON/FOUR/FFH,VI,VE,JHE,VO
DATA RHO,CP/1000.,4200./

```

C

C

C

CALCULATE FILM COEFFICIENTS

```

HE=RHO*CP*VE*ST(FFE)
HI=RHO*CP*VI*ST(FFI)
HH=RHO*CP*VHE*ST(FFH)
HO=RHO*CP*VD*ST(FFO)

```

C

C

C

C

CALCULATE OVERALL HT COEFFICIENT THROUGH CASING

```

      THE NUMBER IN THE NEXT STATEMENT REPRESENTS A SCALE DEPOSIT COEFF.
UC=HO*HI/(HO+HI)
UCF=HO*HE/(HO+HE)
      RETURN
      END

```

C

C

C

C

FUNCTION ST(FF)

CALCULATE STANTON NUMBER

```

PR=1.75
ST=FF/2./(1.0+5.0*SQRT(FF/2.))*(PR-1.0)
      RETURN
      END

```

C

C

```

SUBROUTINE WS
COMMON/ONE/A0,A1,A2,A3,A,AC,AI,AO,AE,B,DC,DEE,DEI,DEO,DH,DLN,DM
COMMON/TWO/XL,FN,FEFF,FFI,FFE,FFO,HI,HH,L,M,MH,TH,TN,TIN,TS,HE
1,T3,D1,D2,CP,TOUT
COMMON/THREE/U,UC,W1,W2,W3,ALPHT,UCF,PLT(100,2),DI,RM,PSI
DATA RHO,G,BETA/1000.,9.8,7.5E-4/
W1=2.*FFO/(PHO*PHO*G*AO*AO*DEO*BETA)
W2=2.*FFI/(RHO*RHO*G*AI*AI*DEI*BETA)*(L-XL)/FLOAT(L)
W3=2.*FFE/(RHO*PHO*G*AE*AE*DEE*BETA)*XL/L
      RETURN
      END

```

C

```

SUBROUTINE FINS
COMMON/ONE/A0,A1,A2,A3,A,AC,AI,AO,AE,B,DC,DEE,DEI,DEO,DH,DLN,DM
COMMON/TWO/XL,FN,FEFF,FFI,FFE,FFO,HI,HH,L,M,MH,TH,TN,TIN,TS,HE
1,T3,D1,D2,CP,TOUT
COMMON/THREE/U,UC,W1,W2,W3,ALPHT,UCF,PLT(100,2),DI,RM,PSI
DATA SCOND/50./
PI=4.*ATAN(1.)

```



```

IF(FN.EQ.0.)GO TO 10
C
C      CALCULATE FIN EFFICIENCY
C
EM=SQRT(2.*HI/SCOND/DLN)
EMB=EM*B
FEFF=TANH(EMU)/EMR
C
SF=FN*(2.*B+DLN)
SO=PI*DH-FN*DLN
GO TO 20
10 FEFF=0.
SF=0.
SO=PI*DH
20 CONTINUE
C
C      CALCULATE OVERALL HT COEF TO DHE
C
U=HH*HE*(SF*FEFF+SO)/(HH*PI*DH+SF*FEFF+SO+HE)
C
C      MODIFY U TO ACCOUNT FOR MULTIPLE TUBES
C
RETURN
END
C
SUBROUTINE COEFS
IMPLICIT REAL (L,M)
COMMON/ONE/A0,A1,A2,A3,A,AC,AI,AO,AE,B,CC,DEE,DEI,DEO,DH,DLN,DW
COMMON/TWO/XL,FN,FEFF,FFI,FFE,FFO,HI,HH,L,M,MH,TH,TN,TIN,TS,HE
1,T3,D1,D2,CP,TOUT
COMMON/THREE/U,UC,W1,W2,W3,ALPHT,UCF,PLT(100,2),DI,RP,PSI
DATA CP/4200./
C
ALPHT=XL/L
TB=RM*T3+(1.-RM)*TS
A3=2.*CP/U/A+1./MH
A2=(1.+MR)/(1.-MR)
A1=2*UC*AC*(1.-ALPHT)/CP+UC*AC*ALPHT/2./CP
A0=(2.-ALPHT)*(TIN-TB)/(W1+W2+W3)
RETURN
END
C
SUBROUTINE SOLVE(A0,A1,A2,A3,X)
F(X)=A0+A1*X+A2*X*X+A3*X*X*X
DF(X)=A1+2.*A2*X+3.*A3*X*X
X=4.
C
C      SOLVE THE EQUATION USING NEWTON'S METHOD
C
10 CONTINUE
XN=X-F(X)/DF(X)
ERR=ABS((XN-X)/XN)
X=XN
IF(ERR.LT.1.E-6)RETURN
GO TO 10
END
C
SUBROUTINE OUTPUT(I,NS)
IMPLICIT REAL (L,M)
COMMON/ONE/A0,A1,A2,A3,A,AC,AI,AO,AE,B,CC,DEE,DEI,DEO,DH,DLN,DW
COMMON/TWO/XL,FN,FEFF,FFI,FFE,FFO,HI,HH,L,M,MH,TH,TN,TIN,TS,HE
1,T3,D1,D2,CP,TOUT
COMMON/THREE/U,UC,W1,W2,W3,ALPHT,UCF,PLT(100,2),DI,RP,PSI

```

```

COMMON/FOUR/FFH,VI,VE,VFE,VO,Q,QMAX,EFF,COSKWH,ENGY
WRITE(7,21)DC,DW,DH,TN,TIN,TOUT,TS,MH,M,XL,L,Q,EFF,PSI,COSKWH,
1ENGY
21 FORMAT(1X,9(F7.3,2X),2(F5.1,2X),F7.3,F6.3,F8.2,F7.4,F10.0)
RETURN
END

C
SUBROUTINE PLOT(J,NP)
COMMON/ONE/AD,A1,A2,A3,A,AC,AI,AO,AE,B,CC,DEE,DEI,DEO,DH,OLN,DW
COMMON/TWO/XL,FN,FEFF,FFI,FFE,FFO,HI,HH,L,M,MH,TH,TN,TIN,TS,HE
1,T3,O1,D2,CP,TOUT
COMMON/THREE/U,UC,W1,W2,W3,ALPHT,UCF,PLT(100,2),DI,RM,PSI
COMMON/FOUR/FFH,VI,VE,VFE,VO,Q,QMAX,EFF,COSKWH,ENGY
DIMENSION VAR(9)
DATA VAR/4HTIN ,3HTS ,3MHM ,3HL ,3HTN ,4HALP ,3HCW ,3HDC ,3HRM /
DATA IFRQ/5/

C
C      RANGEH SETS THE PLOT WIDTH
C      IPLTOP DETERMINES LOWER LIMIT OF PLOT
C      IPLTOP=1 LOWER LIMIT IS 0
C      IPLTOP=2 LOWER LIMIT IS DETERMINED BY RESULT
C
IPLTOP=2
RANGEH=50.

C
C      FIND RANGES OF VARIABLES
C
HMAX=0.
HMIN=0.
IF(IPLTOP.EQ.2)HMIN=PLT(1,2)

C
DO 10 I=1,NR
IF(PLT(I,2).GT.HMAX)HMAX=PLT(I,2)
IF(PLT(I,2).LT.HMIN)HMIN=PLT(I,2)
10 CONTINUE

C
C      DETERMINE SCALE FOR PLOT
C
HMAXS=INT(HMAX/10.)*10+10
HMINS=INT(HMIN/10.)*10-10
IF(HMIN.EQ.0.)HMINS=0.
SCALE=RANGEH/(HMAXS-HMINS)

C
C      WRITE HEADING ON PLOT
C
WRITE(8,11)
11 FORMAT(//40X,15HDHE OUTPUT (KW))
IRNG=RANGEH-6.
NCY=RANGEH/5.
WRITE(8,13)HMINS,IRNG,HMAXS
13 FORMAT(7X,F6.2,=X,F6.2)
WRITE(8,15)VAF(J),NCY
15 FORMAT(4X,A3,3X,(5H*....),1H*)
IT=RANGEH+11.

C
C
C      PLOT RESULTS
C
DO 100 I=1,NP
IPLT2=(PLT(I,2)-HMIN)*SCALE+0.5
IF(MOD(I-1,IFRQ).EQ.0)50,60
50 WRITE(8,101)PLT(I,1),IPLT2,IT

```

```

        GO TO 100
    60  WRITE(8,111)IFLT2,IT
    100 CONTINUE
    101 FORMAT(1X,F7.3,1X,1H*,1X,=X,1HX,T=,1H.)
    111 FORMAT(9X,1H.,=X,1HX,T=,1H.)
        WRITE(8,15)VAR(J),NCY
C
C          PRINT VALUES OF PARAMETERS ON GRAPH
C
        WRITE(8,113)
    113 FORMAT(//)
        IF(J.NE.1.AND.J.NE.6)WRITE(8,121)L,DC,OW
    121 FORMAT(/,3X,LENGTH= ,F7.2, CASING DIAMETER= ,F7.4,
    1  WELLBORE= ,F7.4)
        IF(J.EQ.1)WRITE(8,122)L,OW
    122 FORMAT(/,3X,LENGTH= ,F7.2, WELLBORE= ,F7.4, M)
        IF(J.EQ.6)WRITE(8,123)DC,OW
    123 FORMAT(/,3X,CASING DIAMETER= ,F7.4, WELLBORE= ,F7.4, M)
        IF(J.NE.2.AND.J.NE.3)WRITE(8,124)DH,MH
    124 FORMAT(4X,DHE DIAMETER= ,F7.4,3X,DHE MASS FLOW RATE= ,
    1F6.3)
        IF(J.EQ.2)WRITE(8,125)MH
    125 FORMAT(3X,MASS FLOW RATE THROUGH DHE= ,F6.3, KG/S)
        IF(J.EQ.3)WRITE(8,126)DH
    126 FORMAT(3X,DHE DIAMETER= ,F7.4, M)
        IN=FN
        IF(IN.EQ.0)GO TO 200
        IF(J.NE.4)WRITE(8,127)IN,CLN,B
    127 FORMAT(3X,I3,FIAS ,F7.4, M BY ,F7.4, M LONG)
        IF(J.EQ.4)WRITE(8,128)DLN,B
    128 FORMAT(3X,FIN THICKNESS= ,F7.4, LENGTH= ,F7.4)
    200 CONTINUE
        IN=TN
        IF(J.NE.5)WRITE(8,131)IN
    131 FORMAT(3X,TOTAL DHE LOOPS= ,I4,/)
        IF(J.EQ.5)WRITE(8,132)
    132 FORMAT(/)
    133 RETURN
        END

```